Predicted future (2023-2100) water resource at hydropower potential 06.g and 07.e in Southwest Greenland

Project no.: B24-56

Asiaq Report 2023-27 December 2023

Introduction

The Ministry of Agriculture, Self-sufficiency, Energy and Environment under the Government of Greenland has requested Asiaq and GEUS to provide time series of predicted future water resources for hydropower potential 06.g and 07.e in Southwest Greenland.

To do this we have extracted runoff data for each catchment from regional climate model outputs, and we have evaluated and adjusted the model outputs based on measured runoff.

To give indications of the uncertainty on the predicted water resources we provide data from two different regional climate models forced at the boundaries by two different global climate models and three different future climate scenarios (covering the period 2015-2100). A scenario covering the historic period before 2015 provided model data overlapping with measured data from which adjustment factors are deduced. A schematic of the process chain to produce the time series of predicted future water resources is given in Figure 1.

The choice of combinations of climate scenarios, global and regional climate models have been determined by the model simulations that had already been carried out by the institutions running the models.

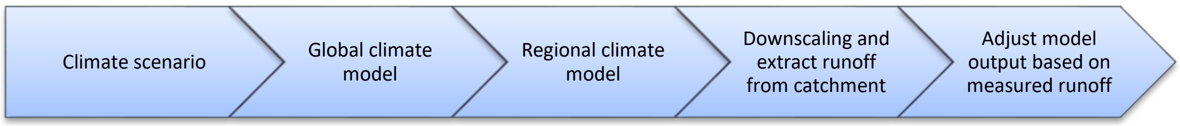

Figure 1 Process chain for providing predicted future water resources.

The work described in this report would not have been possible without access to regional climate model (RCM) outputs, which have been provided for this project free of charge. We would therefore like to acknowledge and thank Xavier Fettweis from University of Liege in Belgium, who has provided data from RCM MAR as well as Martin Olesen and Fredrik Boberg from the Danish Meteorological Institute, who have provided data from RCM HIRHAM.

Prepared by: Dorthe Petersen, Asiaq

Synne Høyer Svendsen, GEUS

Andreas Ahlstrøm, GEUS

Frontpage: outlet river from catchment 06.g.II in early September. Photo by Dorthe Petersen

Content

Appendix

Data files

PredictedFutureRunoff_06gI_2023-2100_AsiaqRapport2023-27.txt
PredictedFutureRunoff_06gII_2023-2100_AsiaqRapport2023-27.txt
PredictedFutureRunoff_06gIII_2023-2100_AsiaqRapport2023-27.txt
PredictedFutureRunoff_06gIV_2023-2100_AsiaqRapport2023-27.txt

PredictedFutureRunoff_07e_2023-2100_AsiaqRapport2023-27.txt

1 Hydropower potential 06.g and 07.e

1.1 Location and catchment areas

The hydropower potentials 06.g and 07.e are situated in Southwest Greenland between Nuuk and Kangerlussuaq, Figure 2. For both hydropower potentials meltwater from the Greenland Ice Sheet (GrIS) is a significant contributor to the water resource. The method used to delineate the catchments is described in GEUS report 2021/45.

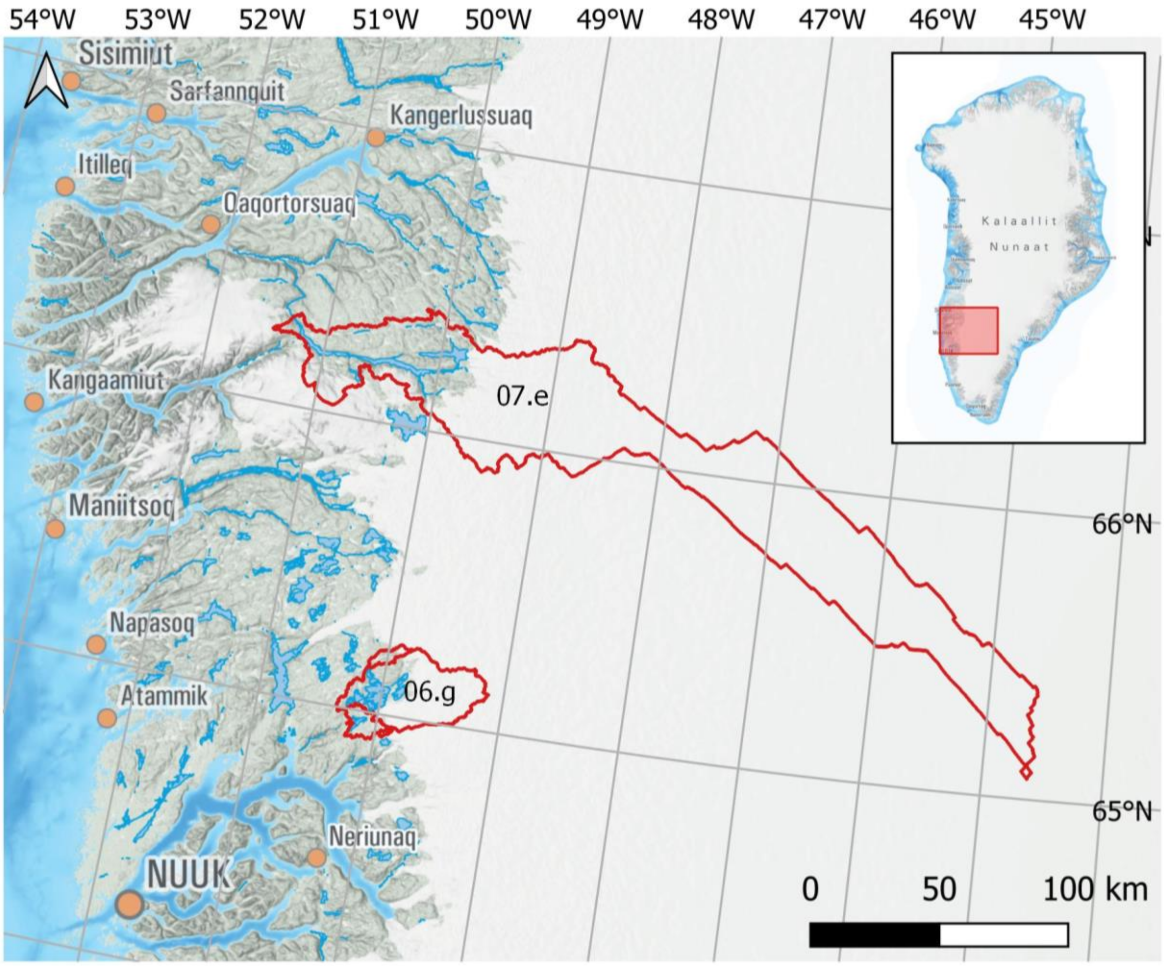

Figure 2 Hydropower potential 06.g and 07.e are situated in Southwest Greenland between Nuuk and Kangerlussuaq. Background map is 'Åbent Land Grønland' provided by the Danish Agency for Data Supply and Infrastructure (SDFI).

Hydropower potential 07.e consists of one natural catchment, whereas hydropower potential 06.g consists of four natural catchments, in the following named 06.g.I, 06.g.II, 06.g.III and 06.g.IV, see Figure 3. All catchments have a glacier covered part, but the glacier covered share (% of total area) differ.

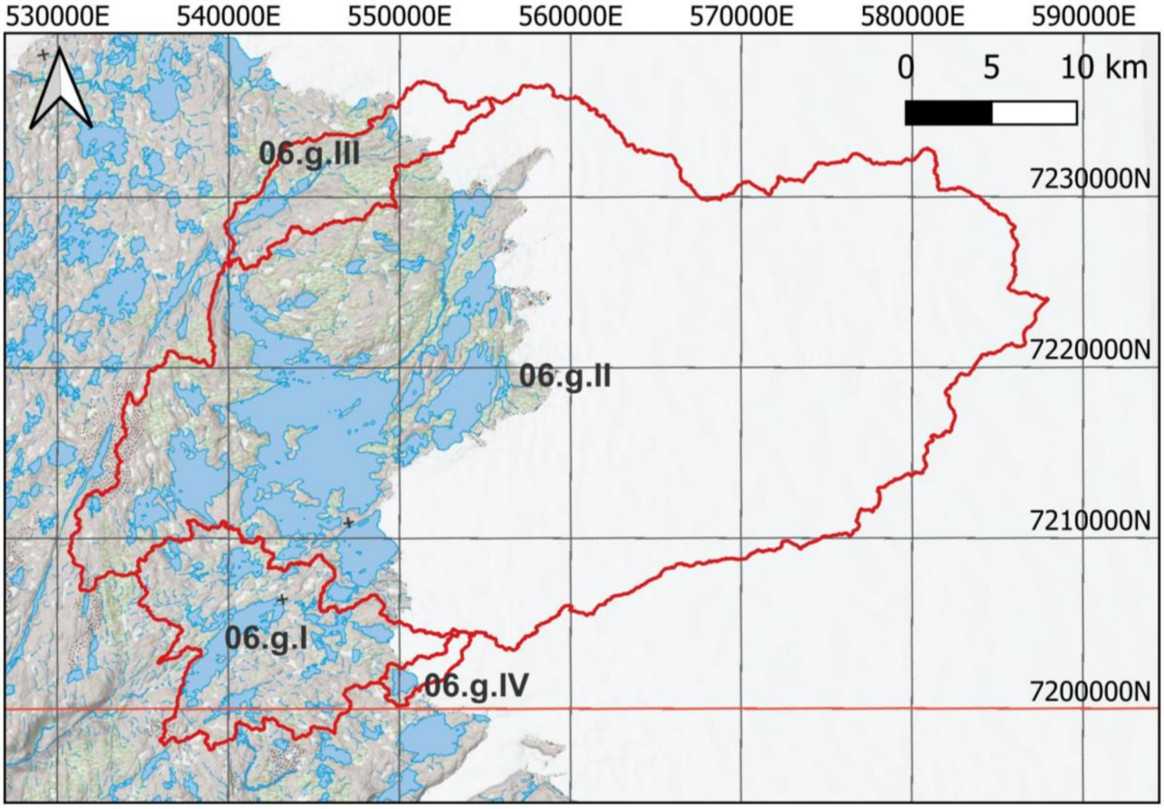

Figure 3 Hydropower potential 06.g consists of four natural catchments. Map coordinates are UTM22N. Background map is 'Åbent Land Grønland' provided by the Danish Agency for Data Supply and Infrastructure (SDFI).

1.2 Measured discharge

The water resource at a location is evaluated from the discharge time series from that location. The discharge time series is not measured directly but calculated indirectly from continuously measured water level and a stage-discharge relation for the location. A stage-discharge relation is an empirical relation describing the discharge as a function of the elevation of the water surface (the water level). A more detailed description of the method can be found in GEUS report 2021/45.

In-situ measurements of discharge have been carried out by Asiaq and/or Asiaq's predecessor the Greenland Technical Organisation (GTO) at all catchments of hydropower potential 06.g and 07.e. However, the length of the measured discharge time series and the quality of the measurements vary between catchments. To give better and more consistent evaluations of the water resource at each catchment, gaps have been filled and terminated measured time series extended with adjusted climate model data or adjusted measured data from neighbouring catchments. Details on the method of gap filling and extensions of time series and the quality of the measured time series can be found in GEUS report 2021/45. An overview of the data coverage of the resulting discharge time series is given in Figure 4.

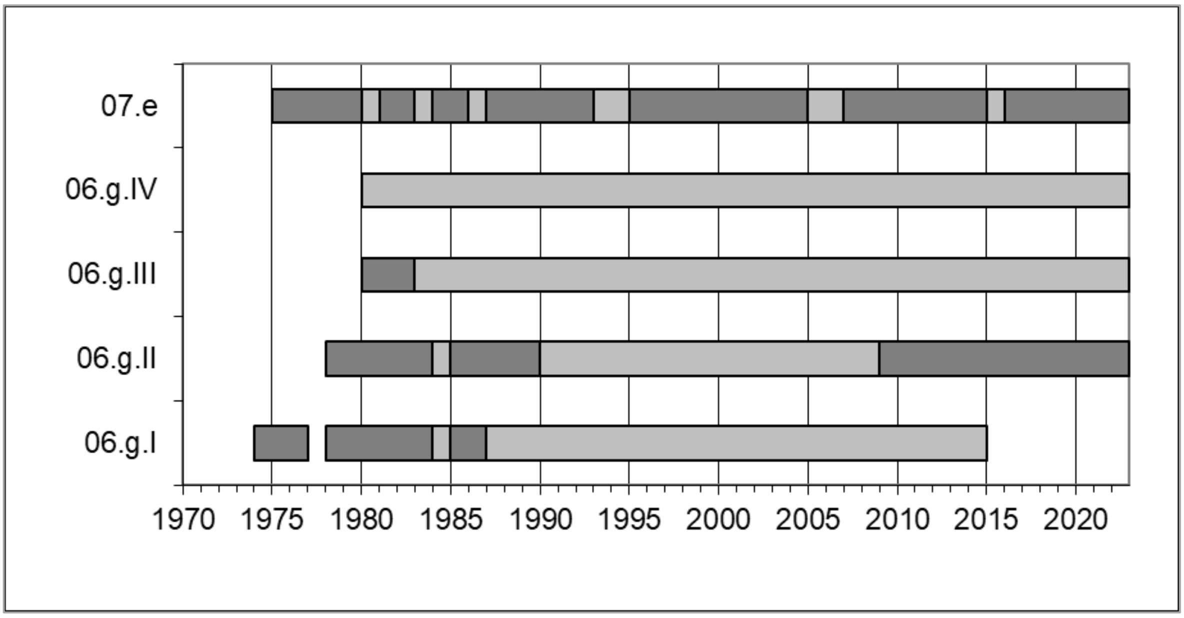

Figure 4 Data coverage of the discharge time series for the catchments of hydropower potential 06.g and 07.e. Years with measured data (dark grey) and years with estimated data, i.e. adjusted model data or adjusted measured data from neighbouring catchments (light grey) are shown.

2 Regional climate model simulations

While discharge calculations based on in-situ observations is the most accurate way to estimate the water resource available for hydropower in a catchment, climate modelling remains the only option when assessing the future evolution of the resource. The interconnected nature of the global climate system requires Global Climate Models (also called General or Global Circulation Models and abbreviated to GCMs) to capture the evolution of the most important parameters. The comprehensive GCM's are by computational necessity relatively coarse in their spatial and vertical resolution, and higher resolution Regional Climate Models (RCMs) are required to resolve processes of importance to the water balance on the scale of hydrological catchments. Climate models do not necessarily agree, neither on the GCM- nor the RCM-scale, and consequently, the choice of models have an impact on the projected water resource availability.

Given the increasing impact of anthropogenically induced climate change, not only the choice of GCM or RCM matters, but also the choice of expected future greenhouse gas emissions. An attempt at capturing the different types of futures we may choose has been made by defining so-called Shared Socioeconomic Pathways (SSPs) (Riahi et al., 2017), used in the IPCC Sixth Assessment Report on climate change (IPCC, 2021). The SSPs constitute climate change scenarios of projected global socioeconomic change up until the year 2100. As such, they provide greenhouse gas emissions scenarios depending on different choices of climate policy. Five main SSPs are defined, summarized as:

- SSP1: Sustainability ("Taking the Green Road")
- SSP2: "Middle of the Road"
- SSP3: Regional Rivalry ("A Rocky Road")
- SSP4: Inequality ("A Road Divided")
- SSP5: Fossil-fueled Development ("Taking the Highway")

These socioeconomic pathways are combined with the Representative Concentration Pathways (RCPs) to describe the future impact on the global climate (van Vuuren et al., 2011). The RCPs were developed to describe different levels of greenhouse gases and other radiative forcings that might occur in the future and are defined by the possible range of radiative forcing values attained in the year 2100 (originally 2.6, 4.5, 6, and 8.5 W/m^2, respectively).

Among different regional climate models (RCMs) there is a noticeable spread in model output. This is caused by differences in the various model schemes. A recent study (Fettweis et al., 2020) comparing modelled ice sheet surface mass balance (SMB) for 13 different models concluded that the largest model spread is found around the margins of the ice sheet, emphasizing the need for continued model development regarding processes related to surface melt and runoff in the ablation zone. The same study showed that the ensemble mean of the models shows the best results when comparing SMB to observations, suggesting that "biases are not systematic among models and that this ensemble estimate can be used as a reference for current climate when carrying out future model development" (Fettweis et al., 2020).

We note that an ensemble mean from several different RCMs provides better agreement with observations than results from a single RCM. However, output from the full range of

SSP-scenarios in a self-consistent RCM framework are very scarce.

This report aims to address some of the variability in projecting the future water resource available for hydropower generation by evaluating model output from two different GCMs (CESM2-CMIP6 and MPI-ESM1-2), and two RCMs (MAR and HIRHAM), using three different SSP-scenarios, namely SSP1-2.6, SSP2-4.5, SSP5-8.5, Table 1.

RCM	MAR		HIRHAM5
GCM	CESM2-CMIP6 (CC)	MPI-ESM1-2 (ME)	CESM2-CMIP6 (CC)
Scenarios	Historical	Historical	Historical
	SSP126	SSP126	
	SSP245	SSP245	
	SSP585	SSP585	SSP585

Table 1 Overview of the 10 different combinations of RCM, GCM and scenarios used to produce the runoff time series for hydropower potential 07.e and 06.g in this report. Historical refers to the period 1950-2014, whereas the SSP-runs cover the period 2015-2100.

3 Regional climate models

3.1 MAR

The regional climate model MAR (Modéle Atmosphérique Régional) (Fettweis, 2007, Fettweis et al., 2013, Fettweis et al., 2017) has been used to downscale the output of two different Global Climate Model (GCM) runs covering the historical period 1950-2014 and three different SSP-scenarios (SSP126, SSP245, SSP585) for the years 2015-2100 (Hofer et al., 2020). These SSP-scenarios are representative of a low emission scenario, a mid-emission scenario and a high-emission scenario, indicating a range of possible emission scenarios (Meinshausen et al., 2020). The GCMs are CESM2-CMIP6 and MPI-ESM1-2. The different SSP-scenarios provide a reasonable spread across possible future scenarios from the very conservative to high-emission scenarios. Using merely two different GCM-drivers cannot provide a full uncertainty estimation but does provide an idea of the sensitivity of MAR to changes in the driving model. Here the two GCMs (CESM2-CMIP6 and MPI-ESM1-2) have been chosen because of the availability of a full suite of scenario runs (historic, SSP126, SSP245 and SSP585) for these GCMs. See Hofer et al. (2020) for estimates of the spread in MAR data depending on the choice of driving GCM.

The present MAR data set allows for a self-consistent (in terms of RCM) comparison between SSP-scenarios, ensuring any differences are caused by differences in climate forcing rather than being the consequence of differences in model biases. In addition, the inclusion of data from MAR simulations driven by two different GCMs allows for rough estimates of any spread due to possible biases in the GCM data.

The native resolution of the MAR simulations is 15 x 15 km (Fettweis et al., 2020). The 15 x 15 km output has subsequently been dynamically downscaled to a 1 km grid as described in Fettweis et al. (2020), the 1 km grid being the standard 1 km grid specified in the protocol for the Ice Sheet Model Intercomparison Project for CMIP6 (Nowicki et al., 2020). The downscaling is performed by a linear interpolation metric of the four nearest inverse-distance-weighted model grid cells (Fettweis et al., 2020). After the downscaling, the interpolated SMB and runoff fields have been corrected for differences between the topography of the native MAR model and the downscaled 1 km grid, using time- and space-varying SMB-elevation gradients (Fettweis et al., 2020, LeClech et al., 2019, Noel et al., 2016, Franco et al., 2012).

3.2 HIRHAM

The regional climate model HIRHAM5 (Christensen et al., 2007, Fettweis et al., 2020) has been run using the Global Climate Model CESM2-CMIP6 for the historical period 1971-2014 and the SSP585 scenario for the years 2015-2100. The available HIRHAM5 dataset is not as comprehensive as the MAR data described previously since only one SSP-scenario (SSP585) is available, however, since the driving GCM model (CESM2-CMIP6) is the same as for one half of the MAR data sets, the available HIRHAM data are most useful in terms of examining variability due to inter-model spread between the different RCMs.

According to Fettweis et al (2020), 'The HIRHAM regional climate model has been developed to include a full surface energy and mass balance model using an original code developed from physical schemes from the ECHAM5 global model and the dynamical schemes from the HIRLAM numerical weather prediction model. It has 31 vertical levels and is forced on 6-hourly intervals on the lateral boundaries. The RCM has a simple five-layer snowpack model to a depth of 10 m over glacier surfaces, incorporating the same parameterizations used in an offline version that has 32 layers.'

For this study, fields of surface mass balance and runoff over ice-covered areas produced by the off-line version of the HIRHAM surface scheme has been made available by DMI. The HIRHAM processing is done closely following the setup for MAR data, although taking into account the differences in the structure of the two model outputs. The differences are mainly concerning the initial time series concatenation and clipping to catchments due to differences in data formats, whereas the subsequent production of annual time series are performed using methods identical to the MAR processing for the surface mass balance and runoff fields.

3.3 Limitations

In the configuration used to produce the present data sets none of the contributing RCMs are coupled to an ice sheet model (Hofer et al., 2020, Langen et al., 2017, Mottram et al., 2017), so simulations are performed with a static ice mask and a static orography. Changes in runoff due to changes in ice extent or dynamics as well as changes in precipitation caused by orographic changes are not addressed. In addition, any glacial water storage (supraglacial lakes, melt ponds, rivers) is not considered, as neither MAR nor HIRHAM resolve this, although HIRHAM5 to some extent addresses meltwater retention and refreezing in the snowpack (Fettweis et al., 2020, Langen et al, 2017, Mottram et al., 2017).

Studies coupling GCMs and ice sheet models show a marked influence on both the ice sheet and the overall climate system (Madsen et al., 2022, Muntjewerf et al., 2020), so the effect of an interactive ice sheet is not negligible. Currently, mostly extreme cases of quadrupling the CO2-concentrations in the atmosphere, either abruptly or by 1 % annual increase, have been studied (Madsen et al., 2022, Muntjewerf et al., 2020), but given the size of the effects of an interactive ice sheet reported by these studies, one may expect significant differences in other, less extreme scenarios as well. The study by Madsen et al. (2022) reports differences in the overall surface mass balance of the Greenland ice sheet as high as 55 % when comparing coupled and uncoupled simulations for the very extreme scenarios quadrupling pre-industrial CO2-levels.

The obvious shortcoming of a non-interactive ice sheet increases the uncertainty of the hydropower potential, but coupled ice-sheet climate models are in their infancy and currently no data sets covering the full range of SSP-scenarios are presently available, not even for global scale models, let alone regional models. For this study, priority has been given to the inclusion of the full spread of SSP-scenarios in a well-tested RCM configuration.

4 Evaluation of regional climate model outputs

We compared the regional climate model outputs with measured data to evaluate the need for adjustment and to decide which adjustment model to choose.

The model simulations used in this project do not aim at describing the exact weather of each year, rather the model aim at describing weather that is likely to happen under the overall climate conditions stipulated by the climate scenarios[1]. Therefore, it is not meaningful to compare model output with measured data on a year-to-year basis. Instead, we compare statistics derived for longer time periods.

The measured runoff data are from the period 1974-2022 (Figure 4), and thus overlaps with the last part of the simulated historic period (hist) and the first part of the future scenarios (SSP scenarios).

4.1 Land runoff versus ice runoff

For the simulations with RCM MAR the runoff from land (not ice-covered) relative to the total runoff is in reasonable agreement with the partitioning estimated from measured precipitation and runoff, Table 2. From the RCM HIRHAM we only had access to modelled runoff from the ice-covered parts of the catchments. The partitioning is relevant as climate change is expected to affect runoff from land differently than runoff from ice-covered areas.

Catchment	Runoff from land (not ice-covered), % of total runoff		
	Estimated from measured data	Model CC MAR	Model ME MAR
07.e	5-15%	12-37%	12-25%
06.g.I	80-100%	89-95%	74-88%
06.g.II	30-35%	32-53%	12-30%

Table 2 The contribution from (not ice-covered) land to the total runoff. Estimates based on measured precipitation and runoff are shown together with results from the model outputs for the three main catchments.

4.2 Magnitude of yearly runoff

Yearly runoff data for the period 1980-2014 (where measured data is available from all catchments) is compared between model and measured data in Figure 5. For four of the five catchments the model mean is much higher than the measured mean (between 25% and 190% higher). For the last catchment (06.g.IV) the model mean is less than the measured mean, however, the measured data from 06.g.IV is uncertain.

The discrepancy between modelled and measured runoff differs between catchments, as well as between models even though all model simulations are under the same climate scenario. This points towards the discrepancies being caused by a combination of multiply error/uncertainty sources, including uncertainty in the catchment delineations especially the ice-covered part, uncertainty of the measured data and gap filling as well as uncertainty and differences in the parameterizations of physical processes and omitted physical processes in the global as well as the regional climate models.

1 This contrasts with re-analysis model-simulations that assimilates measured weather data. However, re-analysis model-simulations can obviously not be used for future predictions.

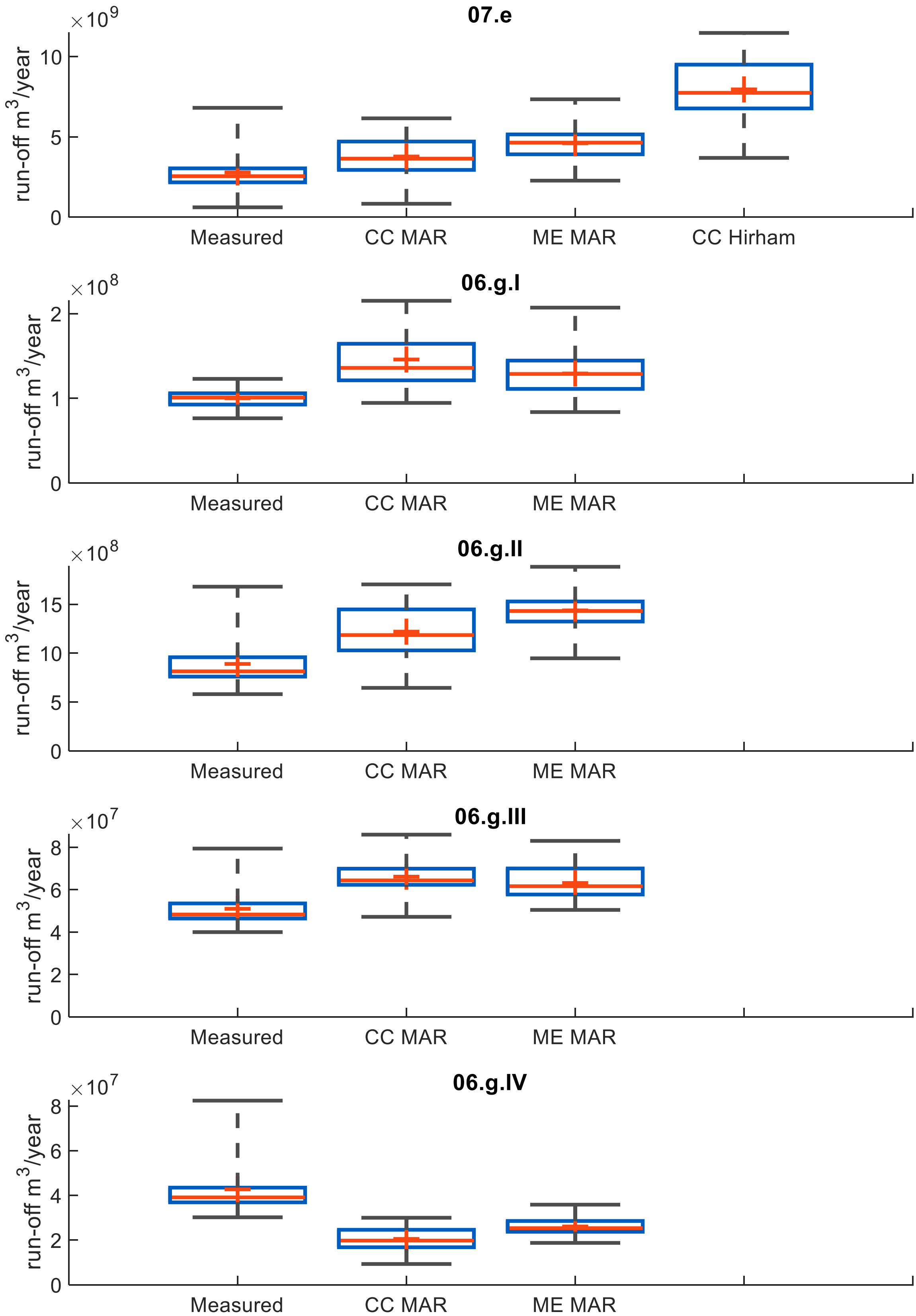

Figure 5 Boxplots of yearly runoff values from the period 1980-2014. Comparison of measured and model runoff for each catchment. In each boxplot the red line is the median, red cross is the mean, the edges of the box are the 25th and 75th percentiles, the whiskers show min and max values.

4.3 Variability of yearly runoff

For the two catchments 07.e and 06.g.II where we have the most complete in-situ measured time series of runoff, measurements show an increase in year-to-year variability around year 2000. None of the models used in this project grasp this change, Figure 6.

In both catchments meltwater from the ice-covered part of the catchment is the dominating contribution to the runoff. Catchments where runoff from land (not covered with ice) dominates, may not experience a similar pattern.

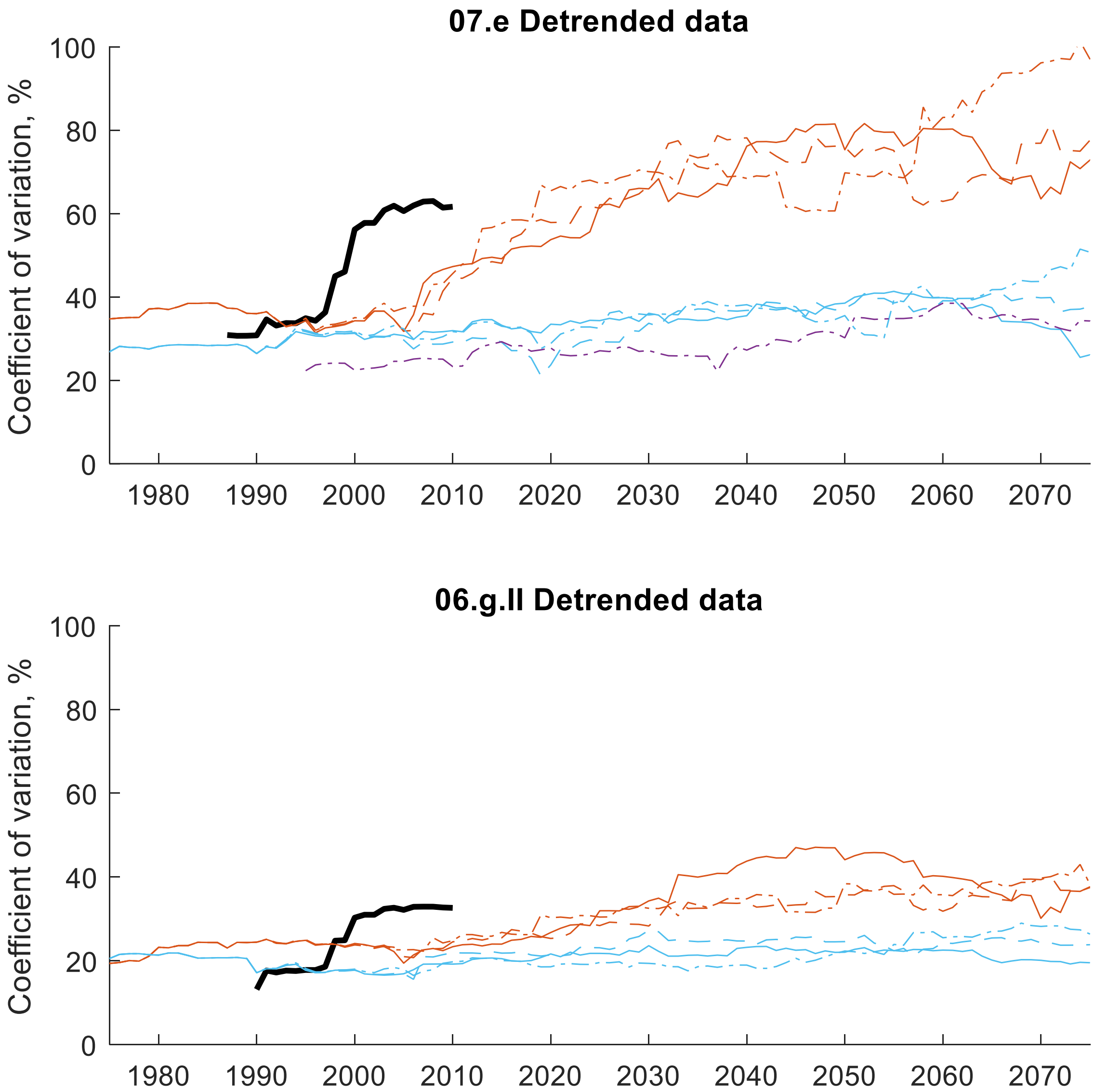

Figure 6 Coefficient of variation calculated for detrended yearly runoff data from catchment 07.e (top panel) and 06.g.II (bottom panel) using a 25-year moving window, with data plotted at the centre of the window. Results from measured runoff (black line) shown together with modelled data from CC MAR (orange), ME MAR (light blue) and CC HIRHAM (lilac). The climate scenario for the future predictions is indicated by the line type; SSP126 as solid line, SSP245 as dashed line, SSP585 as dash-dotted line.

4.4 Monthly distribution of runoff

The time resolution of model data available to this project was monthly data. The distribution of runoff over the year is compared for model and measured data in Figure 7 for the catchments 07.e, 06.g.I and 06.g.II.

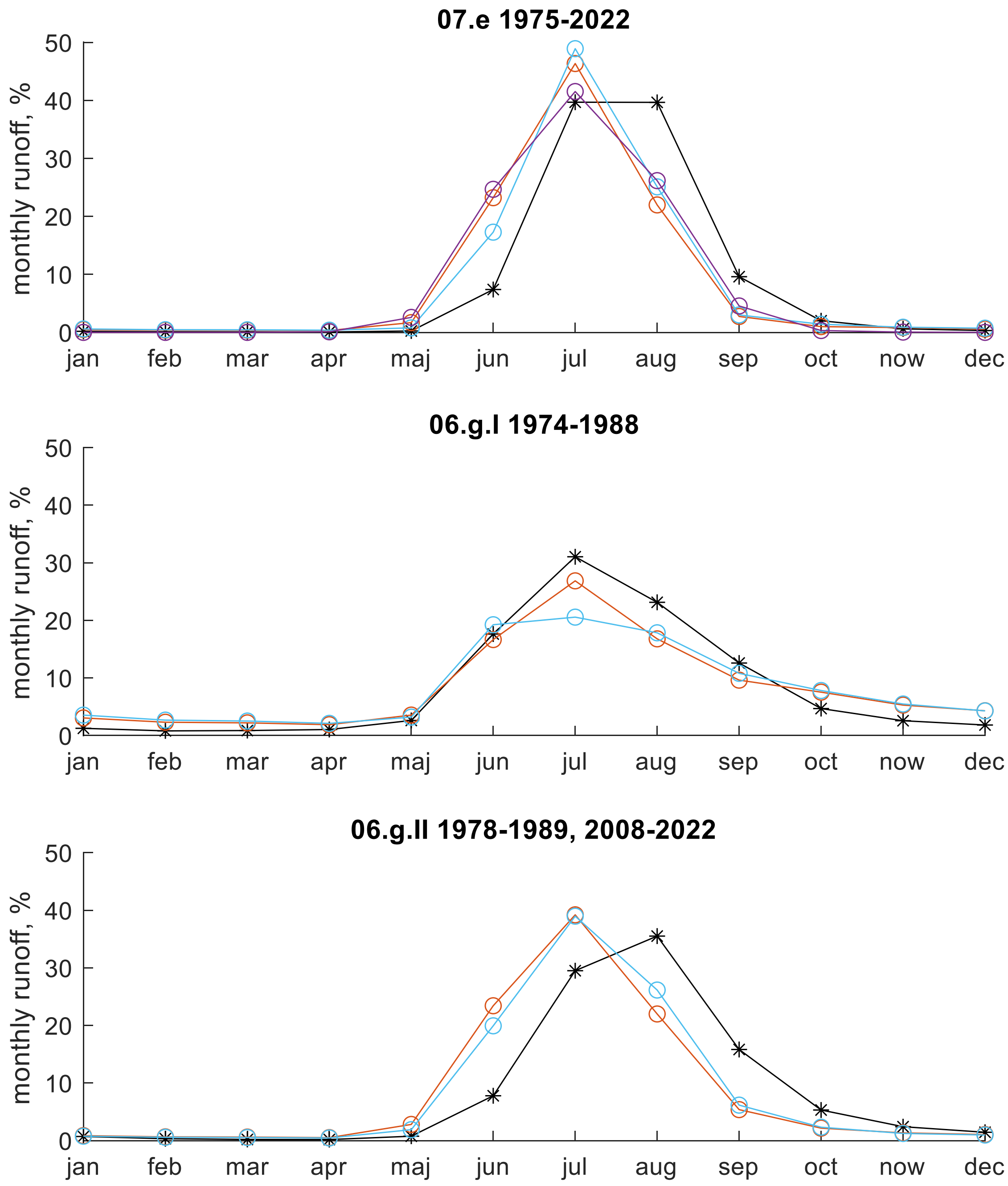

Figure 7 Mean distribution of runoff over the year (% of annual runoff per month) for the periods where measured data exist for the catchments 07.e (top), 06.g.I (middle) and 06.g.II (bottom). The distributions of measured data (black line with stars) are compared with the distribution of model data for CC MAR (orange), ME MAR (light blue) and CC HIRHAM (lilac).

For catchments 06.g.II and 07.e all models predict runoff to occur significantly earlier in the year than the measured runoff. Both 06.g.II and 07.e are catchments that cover a large area (many model grid cells) and where a large part of the catchment is covered by glacier ice. The climate models calculate runoff for each model grid cell but does not include a routing routine. Thus, the travel time for the water to go from each grid cell to the outlet of the catchment (where the in-situ measurements was carried out) is missing in the model output and in the summation of model outputs over the catchment. Further, there might be transport and retardation processes within the snow and glacier ice that are still not adequately described in the models.

For catchment 06.g.I modelled and measured distribution of runoff is in better agreement. The catchment of 06.g.I is considerably smaller than 06.g.II and 07.e (see Figure 2 and Figure 3) and thus the lacking routing routine is less critical.

The model simulations for the future scenarios show a tendency towards a longer runoff season, with a larger part of the yearly runoff occurring in the beginning and the end of the runoff season, see example in Figure 8. The predicted change in the runoff distribution is however small compared to the discrepancy between modelled and measured distribution.

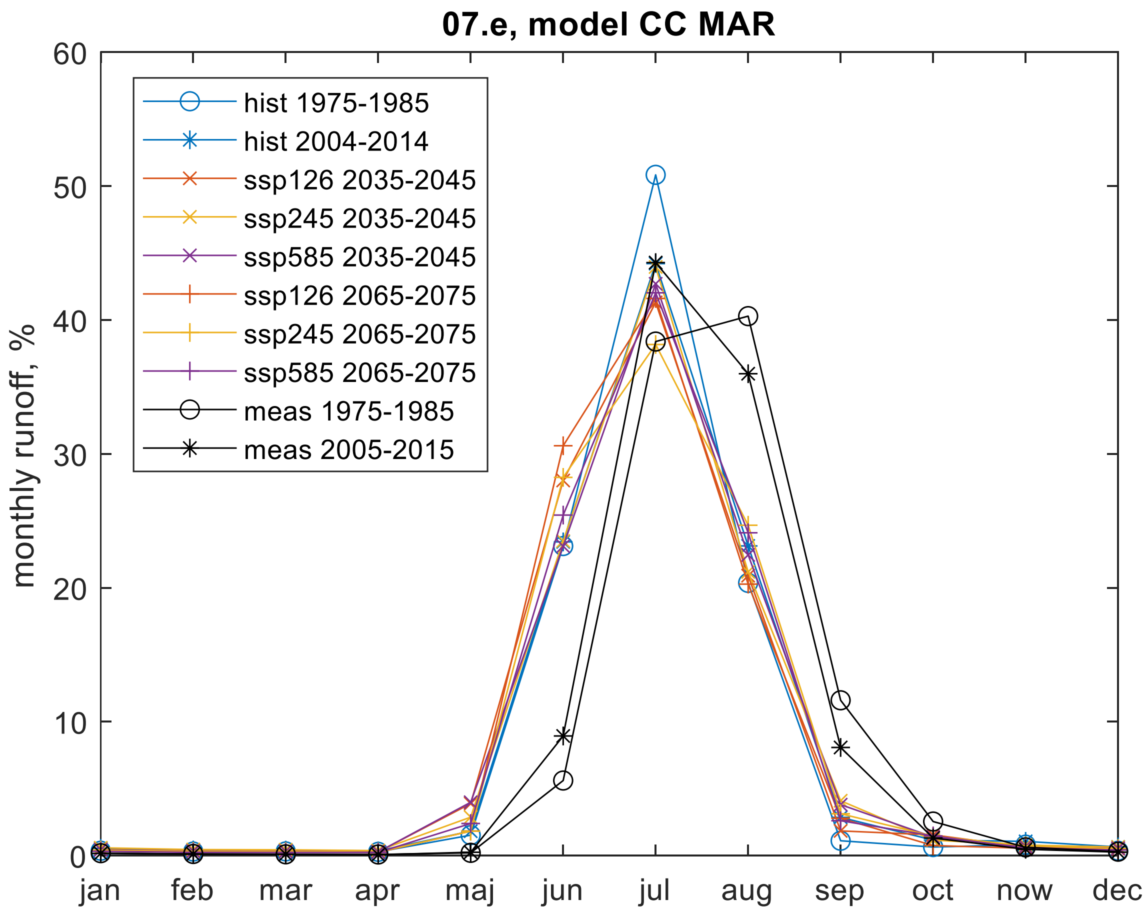

Figure 8 Predicted changes in runoff distribution over the year by CC MAR for catchment 07.e.

5 Adjustment of regional climate model outputs

5.1 Adjustment method

The evaluation of model outputs (section 4) showed that model data needs adjustment to be a reasonable representation of catchment water resources.

The need for adjustment originates from a combination of many sources of uncertainties. The adjustment that we can derive within the scope of this project will not describe specific physical processes but will take the form of an empirical formula, which we will then extrapolate and use for the future scenarios. Therefore, we prioritize to use a simple and transparent adjustment model. We further prioritize to adjust the model to fit the mean annual measured runoff.

The adjustment model consists of multiplying the modelled annual runoff with a constant (an adjustment factor). To find the adjustment factor 25-year moving means of measured data is divided by 25-year moving means of model data. This gives a range for the adjustment factor, and the minimum and maximum value are extracted. Adjustment factors are derived for each combination of models (GCM and RCM) and for each catchment.

5.2 Adjustment factors

A list of the applied adjustment factors is shown in Table 3.

Catchment	ME MAR		CC MAR		CC HIRHAM	
	AF min	AF max	AF min	AF max	AF min	AF max
07.e	0.50	0.67	0.68	0.77	0.30	0.37
06.g.I	0.76	0.81	0.66	0.73		
06.g.II	0.57	0.64	0.66	0.74		
06.g.III	0.77	0.84	0.74	0.80		
06.g.IV	1.50	1.79	1.97	2.07		

Table 3 Overview of adjustment factors (AF) used to adjust modelled annual runoff values. Individual adjustment factors are used for each catchment and for each combination of global climate model (GCM) and regional climate model (RCM). For each combination of climate models, a minimum and a maximum adjustment factor is used.

5.3 Deliverables

The data files provided together with this report contains the adjusted model results of annual runoff for each catchment, each model combination and each of the future scenarios adjusted by a minimum and a maximum adjustment factor, respectively. The adjusted data covers the years 2023-2100. There is a data file for each catchment, and the catchment name appear in the file name.

The files include a header line. The naming convention used for the time series (columns) in the data files is:
<Catchment>\<SSP scenario>\<global climate model abbreviation>\<regional climate model>\<Adjustment factor min/max>,
e.g. '07.e\SSP126\CC\MAR\AFmin'.

Note that the adjustment model seeks to fit the mean annual runoff to measurements. Based on the evaluation of model output we do not expect the adjusted model result to truthfully depict year-to-year variability and changes in year-to-year variability in runoff (see section 4.3)

We do not provide monthly data. If monthly data is needed, we recommend calculating runoff distributions (% runoff per month) from the measured time series and apply these to the adjusted model data.

6 Predicted future water resource

The adjusted model results are compared for hydropower potential 07.e in Figure 9 and for hydropower potential 06.g (runoff from the four catchments summed) in Figure 10.

The models predict that the future water resource will be at the same level or higher than the present, i.e. the most recent period. The model simulations driven by the different SSP scenarios tends to diverge more as time progresses, which is to be expected from the stipulated development in greenhouse gas emissions within the scenarios.

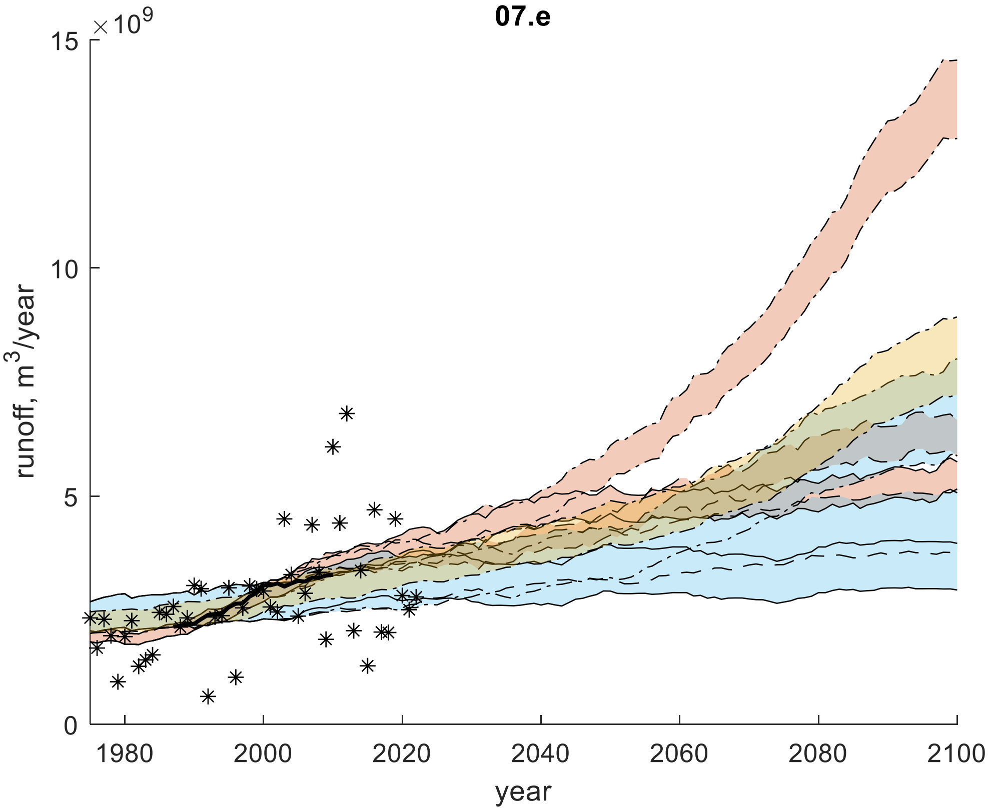

Figure 9 Adjusted model results for hydropower potential 07.e shown as 25-year moving means. The coloured bands show the span of adjustment for each model simulation using the minimum and maximum adjustment factor, respectively. Model simulations with model CC MAR (red), ME MAR (blue) and CC HIRHAM (yellow) are shown. The type of line bordering the coloured bands indicates the SSP scenario; SSP126 as solid line, SSP245 as dashed line, SSP585 as dash-dotted line. The black stars are measured yearly runoff.

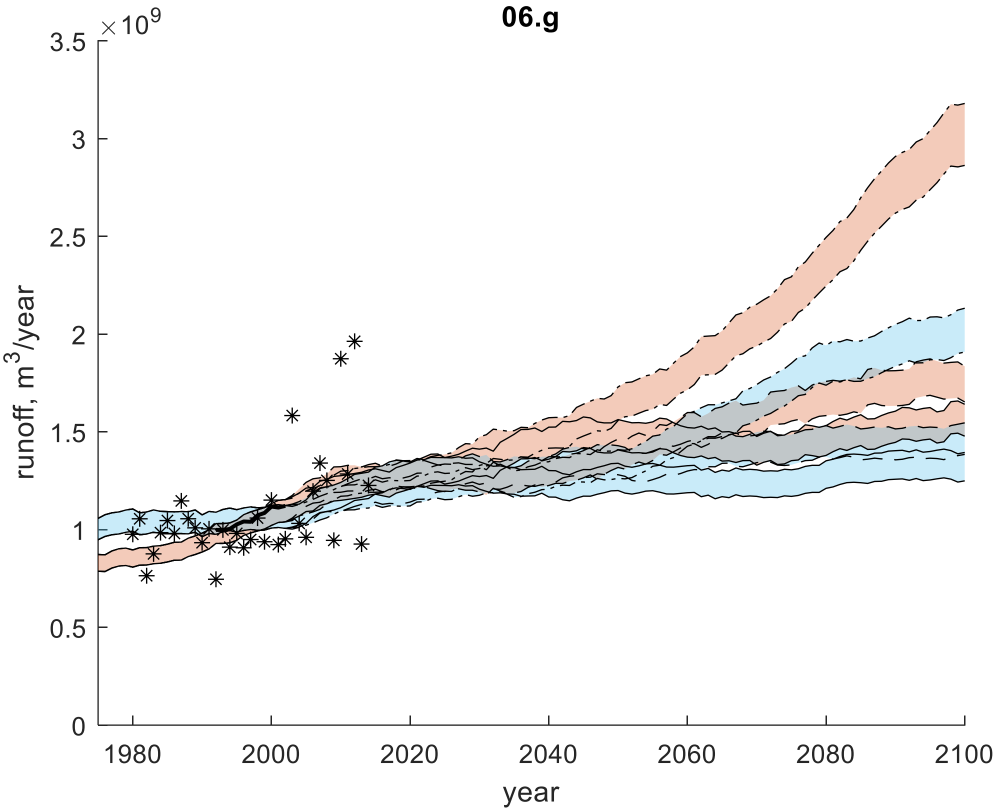

Figure 10 Adjusted model results for hydropower potential 06.g (runoff from the four catchments summed) shown as 25-year moving means. The coloured bands show the span of adjustment for each model simulation using the minimum and maximum adjustment factor, respectively. Model simulations with model CC MAR (red) and ME MAR (blue) are shown. The type of line bordering the coloured bands indicates the SSP scenario; SSP126 as solid line, SSP245 as dashed line, SSP585 as dash-dotted line. The black stars are measured yearly runoff.

For both hydropower potentials the model simulations driven by the global model CESM2-CMIP6 (CC) tends to give higher runoff values than simulations driven by the global model MPI-ESM1 (ME). The higher runoff is most likely attributed to differences in temperature and precipitation. Considering 10-year means of the annual temperature and precipitation cycles for the various catchments all hint towards the CESM2-driven scenarios being warmer than the MPI-driven scenarios, the tendency being most pronounced in the later part of the time series and for the warmest (SSP585) scenario. Likewise, the precipitation follows the same pattern; we see both a heightening of the monthly totals (Figure 11), but also a shift in precipitation type towards more rain, where we see both an increase in total values and a broadening of the rain peak in the precipitation distribution (Figure 12). These changes are more pronounced in the CESM2-driven scenarios compared to the MPI scenarios. MPI is known to have a negative sea surface temperature bias in the Nordic seas as well as a total precipitation low bias and an air temperature (at 2m above terrain) low bias over Greenland (Müller et al 2018) while known biases for CESM2 includes ‘excessive rainfall in the south, likely associated with unresolved topography, excessive rainfall (van Kampenhout et al., 2019), and a generally too positive SMB bias in the North’ for Greenland (Danabasoglu et al., 2020).

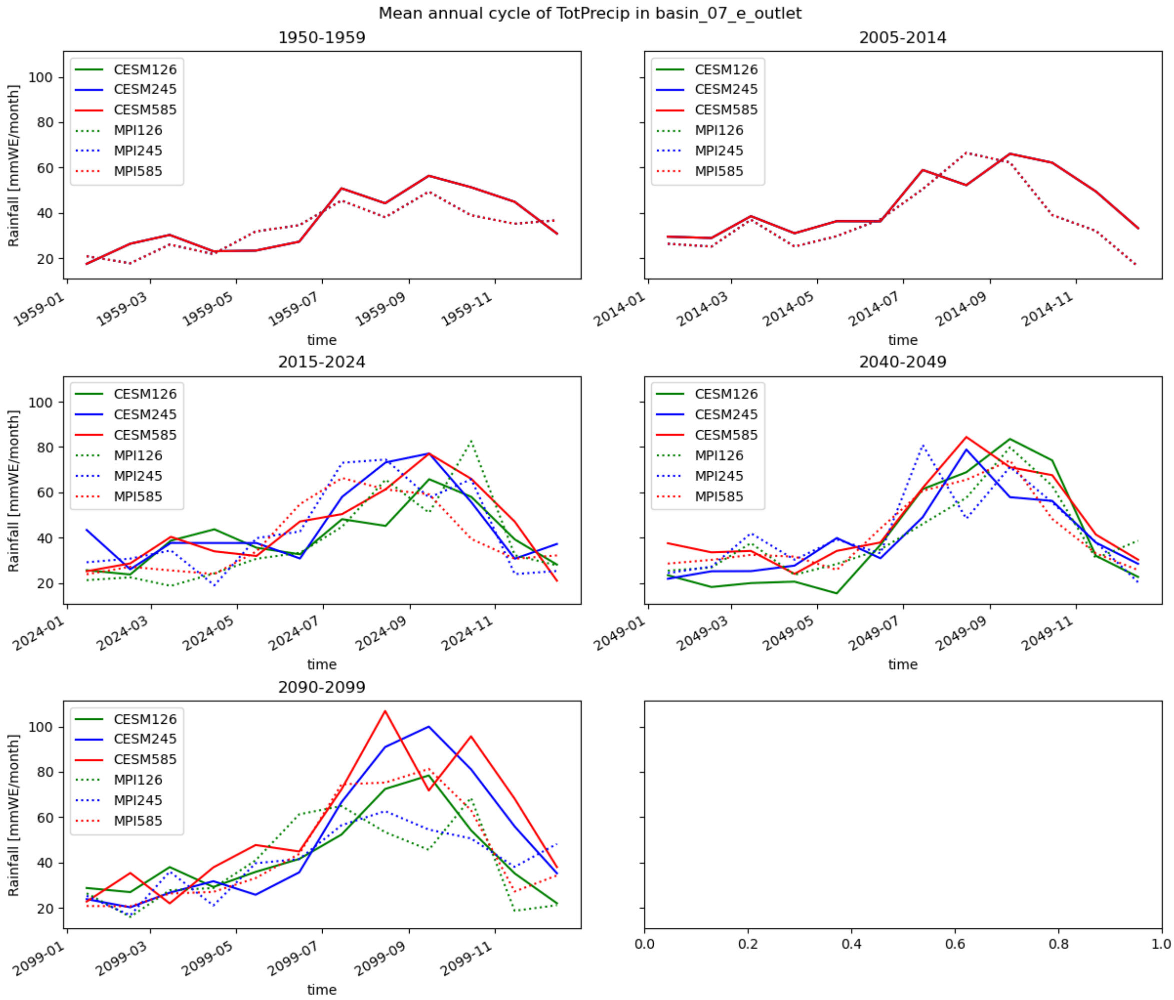

Figure 11 The monthly total precipitation in 07.e, taken as decadal means for representative decades.

The relative change in runoff from present day to 2100 is larger for hydropower potential 07.e than for hydropower potential 06.g, especially in the warmest climate scenario (SSP585). For both hydropower potentials the models predict an increase in the runoff from land as well as in the runoff from ice (Appendix A), but the increase in runoff from the ice-covered part of the catchments is by far the largest contribution.

With the increase in temperature the melt on the ice sheet will intensify and melt will start to occur at higher and higher elevation. For 07.e this means that a large area in the upper part of the catchment, which at precent is in the accumulation zone, will be activated and start to contribute with meltwater (Figure A.1 in Appendix A). The 06.g catchment do not reach so far up on the ice sheet and therefore the relative increase is not as immense (Figure A.3 in Appendix A).

It is important to note that the delineation of the upper part of the 07.e catchment is uncertain and sensitive to changes in the ice surface that may occur as melt in these upper regions become more common. Thus, the actual change in the water resource for 07.e in a much warmer climate could be both less or more than predicted by the models.

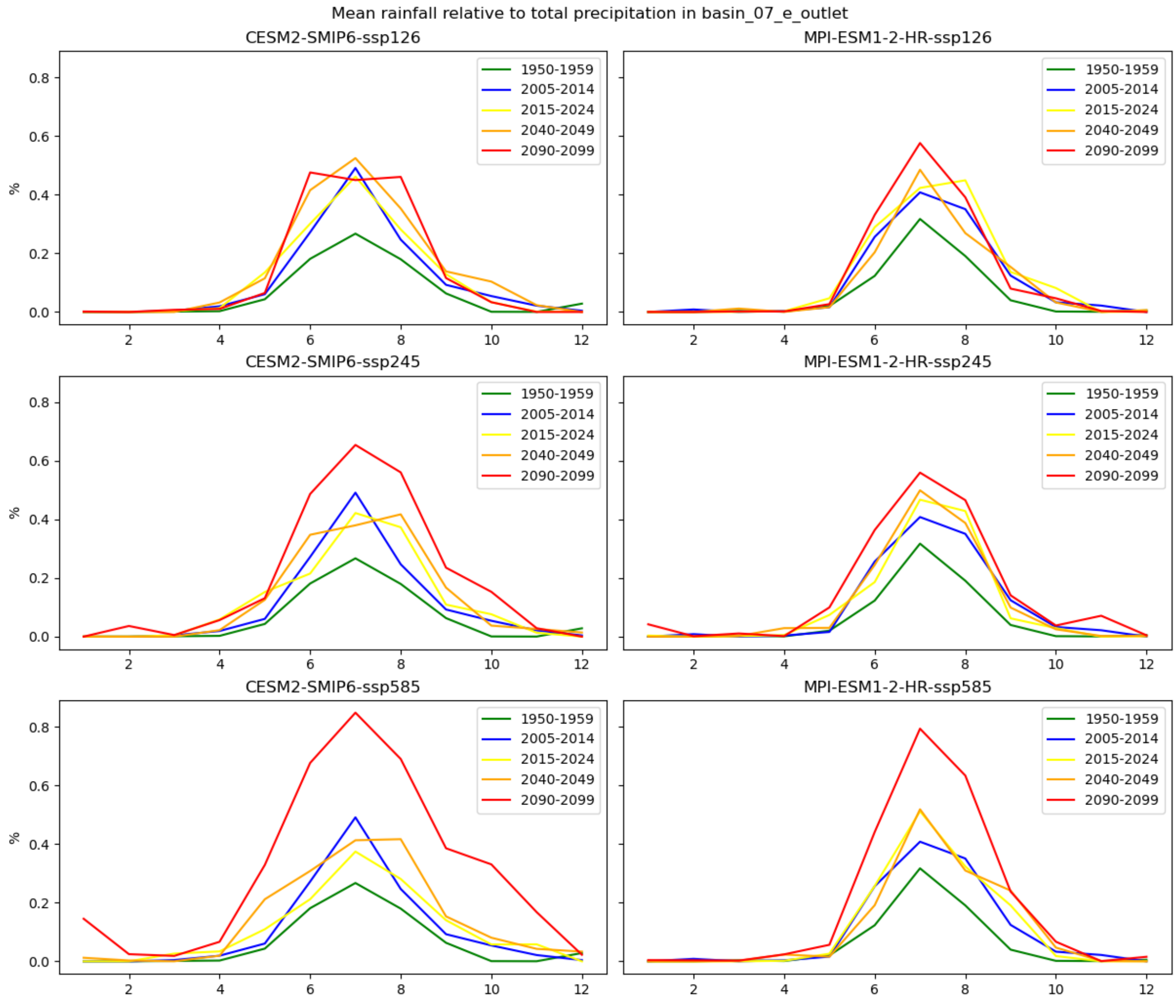

Figure 12 The monthly share of precipitation falling as rain in catchment 07.e predicted by the RCM MAR, for different GCM model forcings and SSP-scenarios.

7 Conclusion

Data files with predicted future (2023-2100) annual runoff values for each of the catchments making up hydropower potential 07.e and 06.g are delivered together with this report.

Monthly runoff data is not provided. If monthly data is needed, we recommend calculating runoff distributions (% runoff per month) from the measured time series and apply these to the adjusted model data.

Model outputs from two different regional climate models run under a combination of three different climate scenarios and two different global climate models have been used. In total seven model simulations were available for hydropower potential 07.e and six model simulations were available for hydropower potential 06.g.

The model output did not directly agree with measured runoff (in the historic period 1974-2022). To improve the results model outputs was multiplied with a minimum and a maximum adjustment factor derived for each catchment and model combination.

The adjusted model outputs seek to fit the mean annual (25-year means) runoff to measurements. Based on the evaluation of model output we do not expect the adjusted model result to truthfully depict year-to-year variability and changes in year-to-year variability in runoff.

The models predict that the future water resource will be at the same level or higher than the present i.e. the most recent period.

8 References

Christensen, O.B., Drews, M., Christensen, J.H., Dethloff, K., Ketelsen, K., Hebestadt, I., and Rinke, A. The HIRHAM regional climate model version 5 (beta). Technical Report 06-17, Danish Meteorological Institute, 2007.

Fettweis, X. Reconstruction of the 1979-2006 Greenland ice sheet surface mass balance using the regional climate model MAR. The Cryosphere, 1(1):21-40, 2007.

Fettweis, X., B. Franco, M. Tedesco, J. H. van Angelen, J. T. M. Lenaerts, M. R. van den Broeke, and H. Gallée. Estimating the Greenland ice sheet surface mass balance contribution to future sea level rise using the regional atmospheric climate model MAR. The Cryosphere, 7(2):469-489, 2013.

Fettweis, X., J. E. Box, C. Agosta, C. Amory, C. Kittel, C. Lang, D. van As, H. Machguth, and H. Gallée. Reconstructions of the 1900-2015 Greenland ice sheet surface mass balance using the regional climate MAR model. The Cryosphere, 11(2):1015-1033, 2017.

Fettweis, X., S. Hofer, U. Krebs-Kanzow, C. Amory, T. Aoki, C. J. Berends, A. Born, J. E. Box, A. Delhasse, K. Fujita, P. Gierz, H. Goelzer, E. Hanna, A. Hashimoto, P. Huybrechts, M.-L. Kapsch, M. D. King, C. Kittel, C. Lang, P. L. Langen, J. T. M. Lenaerts, G. E. Liston, G. Lohmann, S. H. Mernild, U. Mikolajewicz, K. Modali, R. H. Mottram, M. Niwano, B. Noël, J. C. Ryan, A. Smith, J. Stre°ng, M. Tedesco, W. J. van de Berg, M. van den Broeke, R. S. W. van de Wal, L. van Kampenhout, D. Wilton, B. Wouters, F. Ziemen, and T. Zolles. GrSMBMIP: intercomparison of the modelled 19802012 surface mass balance over the Greenland Ice Sheet. The Cryosphere, 14(11):39353958, 2020.

Franco, B., Fettweis, X., Lang, C., and Erpicum, M.: Impact of spatial resolution on the modelling of the Greenland ice sheet surface mass balance between 1990–2010, using the regional climate model MAR, The Cryosphere, 6, 695–711, https://doi.org/10.5194/tc-6-695-2012, 2012.

Ganabasoglu, G., J.-F. Lamarque, J. Bacmeister, D.A. Bailey, A.K. DuVivier, J. Edwards, L.K. Emmons, J. Fasullo, R. Carcia, A. Gettelman, C. Hannay, M.M. Holland, W.G. Large, P.H. Lauritzen, D.M. Lawrence, J.T.M. Lenaerts, K. Lindsay, W.H. Lipscomb, M.J. Mills, R. Neale, K.W. Oleson, B. Otte-Bliesner, A.S. Phillips, W. Sacks, S. Tilmes, L. van Kampenhout, M. vertenstein, A. Bertini, J. Dennis, C. Deser, C. Fischer, B. Fox-Kemper, J.E. Kay, D. Kinnison, P.J. Kushner, V.E. Larson, M.C. Long, S. Mickelson, J.K. Moore, E. Nienhouse, L. Polvani, R.J. Rasch, W.G. Strand: The Community Earth System Model Version 2 (CESM2). Journal of Advances in Modeling Earth Systems, vol 12, 2, 2020. DOI: https://doi.org/10.1029/2019MS001916.

GEUS report 2021/45 Evaluation of the water resource for sixteen hydropower potentials of industrial interest in Greenland.

Hofer, S., C. Lang, C. Amory, C. Kittel, A. Delhasse, A. Tedstone, and X. Fettweis. Greater Greenland Ice Sheet contribution to global sea level rise in CMIP6. Nature Communications, 6289(11), 2020.

IPCC, 2021: Summary for Policymakers. In: Climate Change 2021: The Physical Science Basis. Contribution of Working Group I to the Sixth Assessment Report of the Intergovernmental Panel on Climate Change [Masson-Delmotte, V., P. Zhai, A. Pirani, S.L. Connors, C. Péan, S. Berger, N. Caud, Y. Chen, L. Goldfarb, M.I. Gomis, M. Huang, Leitzell, K., E. Lonnoy, J.B.R. Matthews, T.K. Maycock, T. Waterfield, O. Yelekçi, R. Yu, and B. Zhou (eds.)]. Cambridge University Press, Cambridge, United Kingdom and New York, NY, USA, pp. 3−32, doi:10.1017/9781009157896.001.

Le clec'h, S., Charbit, S., Quiquet, A., Fettweis, X., Dumas, C., Kageyama, M., Wyard, C., and Ritz, C.: Assessment of the Greenland ice sheet–atmosphere feedbacks for the next century with a regional atmospheric model coupled to an ice sheet model, The Cryosphere, 13, 373–395, https://doi.org/10.5194/tc-13-373-2019, 2019.

Madsen, M.S., Yang, S., Aðalgeirsdóttir, G. et al. The role of an interactive Greenland ice sheet in the coupled climate-ice sheet model EC-Earth-PISM. Clim Dyn 59, 1189–1211 (2022). https://doi.org/10.1007/s00382-022-06184-6.

Meinshausen, M., Z. R. J. Nicholls, J. Lewis, M. J. Gidden, E. Vogel, M. Freund, U. Beyerle, C. Gessner, A. Nauels, N. Bauer, J. G. Canadell, J. S. Daniel, A. John, P. B. Krummel, G. Luderer, N. Meinshausen, S. A. Montzka, P. J. Rayner, S. Reimann, S. J. Smith, M. van den Berg, G. J. M. Velders, M. K. Vollmer, and R. H. J. Wang. The shared socio-economic pathway (SSP) greenhouse gas concentrations and their extensions to 2500. Geoscientific Model Development, 13(8):3571-3605, 2020.

Mottram, R., F. Boberg, P. Langen, S. Yang, C. Rodehacke, J.H. Christensen, M.S. Madsen: Surface mass balance of the Greenland ice sheet in the regional climate model HIRHAM5: Present state and future prospects. Low Temperature Science 75, p 105-115, 2017. DOI: https://doi.org/10.14943/lowtempscie.75.105.

Müller, W.A., J.H. Jungclaus, T. Mauritsen, J.Baehr, M. Bittner, R. Budich, F. Bunzel, M. Esch, R. Ghosh, H. Haak, T. Ilyina, T. Kleine, L. Kornblues, H. Li, K. Modali, D. Notz, H. Pohlmann, E. Roeckner, I. Stemmler, F. Tian, and J. Marotzke: A Higher-resolution Version of the Max Planck Institute Earth System Model (MPI-ESM1.2-HR). Journal of Advances in Modeling Earth Systems Vol 10, issue 7, 1383-1413, July 2018. DOI: https://doi.org/10.1029/2017MS001217.

Muntjewerf, L., Petrini, M., Vizcaino, M., Ernani da Silva, C., Sellevold, R., Scherrenberg, M. D. W., et al. (2020). Greenland Ice Sheet contribution to 21st century sea level rise as simulated by the coupled CESM2.1-CISM2.1. Geophys. Res. Lett. 47, e2019GL086836. doi:10.1029/2019GL086836.

Noël, B., W. J. van de Berg, H. Machguth, S. Lhermitte, I. Howat, X. Fettweis, and M. R. van den Broeke. A daily, 1 km resolution data set of downscaled greenland ice sheet surface mass balance (19582015). The Cryosphere, 10(5):23612377, 2016.

Nowicki, S., H. Goelzer, H. Seroussi, A. J. Payne, W. H. Lipscomb, A. Abe-Ouchi, C. Agosta, P. Alexander, X. S. Asay-Davis, A. Barthel, T. J. Bracegirdle, R. Cullather, D. Felikson, X. Fettweis, J. M. Gregory, T. Hattermann, N. C. Jourdain, P. Kuipers Munneke, E. Larour, C. M. Little, M. Morlighem, I. Nias, A. Shepherd, E. Simon, D. Slater, R. S.

Smith, F. Stra-neo, L. D. Trusel, M. R. van den Broeke, and R. van de Wal. Experimental protocol for sea level projections from ISMIP6 stand-alone ice sheet models. The Cryosphere, 14(7):2331 2368, 2020.

Riahi, K., van Vuuren, D.P., Kriegler, E., Edmonds, J., O'Neill, B., Fujimori, S., Bauer, N., Calvin, K., et al. (2017). The shared socioeconomic pathways and their energy, land use, and greenhouse gas emissions implications: An overview. Global Environmental Change 42 153-168. https://doi.org/10.1016/j.gloenvcha.2016.05.009.

Van Kampenhout, L., A.M. Rhoades, A.R. Herrington,, C.M. Zarzycki, J.T.M. Lenaerts, W.J. Sacks, M.R. van den Broeke: Regional grid refinement in an Earth system model: Impacts on the simulated Greenland surface mass balance. The Cryosphere, 2019. DOI: https://doi.org/10.5194/tc-13-1547-2019.

Van Vuuren, D.P., Edmonds, J., Kainuma, M. et al. The representative concentration pathways: an overview. Climatic Change 109, 5 (2011). https://doi.org/10.1007/s10584-011-0148-z.

Appendix A: Maps of distributed runoff from RCM MAR

Figure A.1: Distributed runoff from the ice-covered part of the 07.e catchment. Mean value for two time-slices (2015-2024) and (2090-2099).

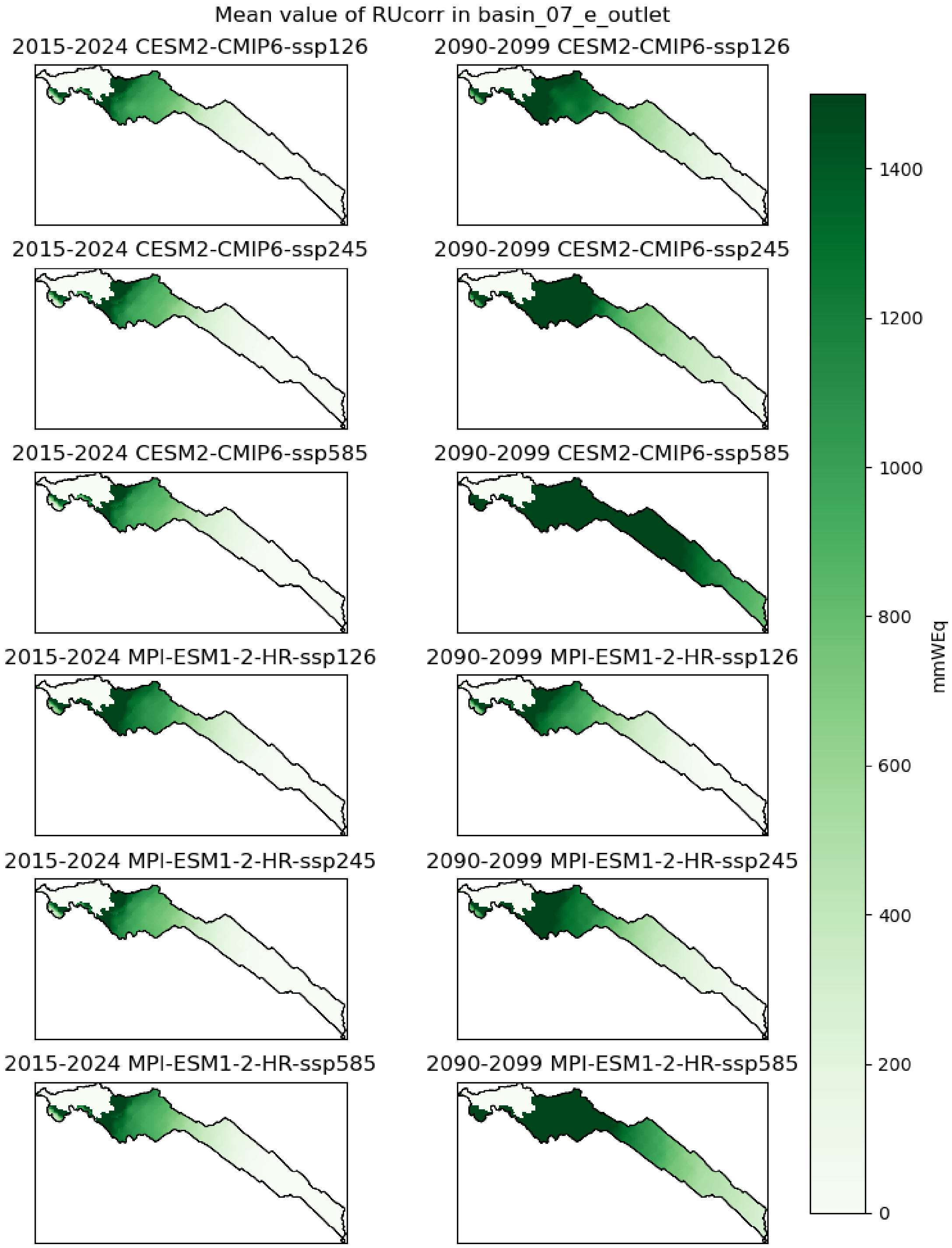

Figure A.2: Distributed runoff from the land part not covered with ice of the 07.e catchment. Mean value for two time-slices (2015-2024) and (2090-2099).

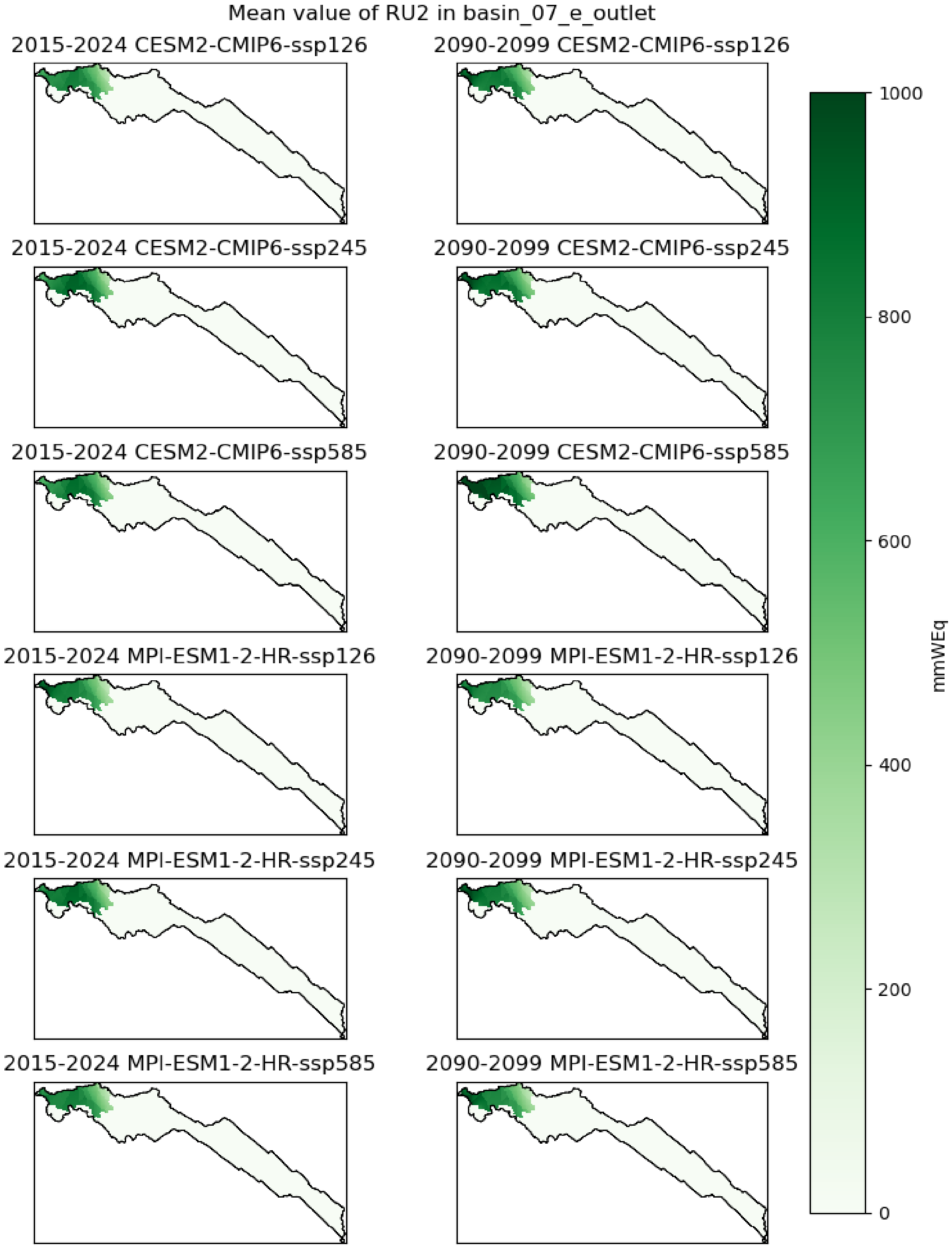

Figure A.3: Distributed runoff from the ice-covered part of the 06.g.II catchment. Mean value for two time-slices (2015-2024) and (2090-2099).

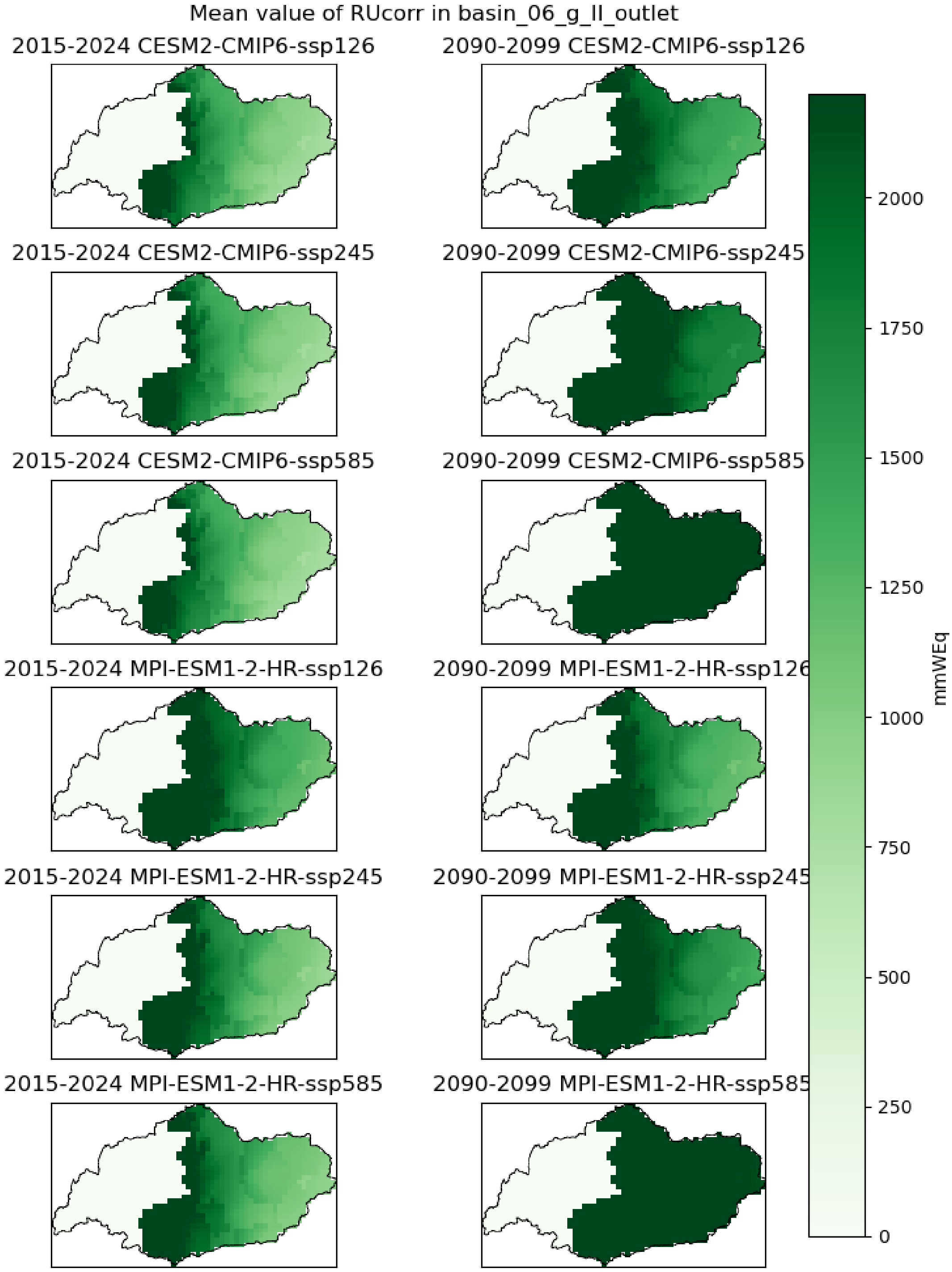

Figure A.4: Distributed runoff from the land part not covered with ice of the 06.g.II catchment. Mean value for two time-slices (2015-2024) and (2090-2099).